Supplementary Information

S.I.1. Testing for the effect of composition treatment on fecundity

We tested for the effect of composition treatment (solo / exotic-dominated / native-dominated / monoculture / control) on individual plant fecundity using a negative binomial model with the function manyglm from the package mvabund in R (Wang et al., 2012; R Development Core Team, 2016). We ran a separate GLM for each focal species. Given that our annual plant population model accounts for neighbour density and identity, we wanted to test whether composition treatment had a further effect on plant fecundity. We therefore included the effects of neighbour density and identity when testing for composition treatment.

For each focal species, the model formula was as described as follows:

$$\textit{Focal species fitness} \sim N_A + N_H + N_W + N_T + N_N + \textit{composition treatment}$$

where N_A, N_H, N_W, N_T and N_N refer to the abundances of *A. calendula*, *H. glabra, W. acuminata, T. cyanopetala*, and all neighbours (combined) which were not any of the four focal species (N_N), respectively. Results from a Wald test on the model outputs for each focal species is presented in Supplementary Table 1. Composition treatment was only found to have a significant effect on *T. cyanopetala,* we hence felt comfortable not including composition treatment as an effect in our study.

Supplementary Table 1.1: Walt test results and associated *p* values testing the effect of neighbour density (N_A, N_H, N_W, N_T and N_N) and neighbourhood composition treatment ('Composition') on the individual fecundity of each focal species (measured as the number of seeds produced). The Walt test was performed using the anova.manyglm function of the mvabund package (Wang et al., 2012) on the results of a negative binomial glm. *p* values below 0.05 are bolded.

	A. calendula			*H. glabra*			*W. acuminata*			*T. cyanopetala*		
	df (df_{res})	Wald test	p	df (df_{res})	Wald test	p	df (df_{res})	Wald test	p	df (df_{res})	Wald test	p
N_A	1 (250)	0.610	0.534	1 (273)	0.051	0.959	1 (272)	0.338	0.757	1 (223)	1.684	0.150
N_H	1 (249)	1.362	0.177	1 (272)	1.637	0.126	1 (271)	1.300	0.195	1 (222)	1.922	0.098
N_W	1 (248)	3.012	**0.007**	1 (271)	5.694	**0.001**	1 (270)	2.177	0.031	1 (221)	2.309	**0.042**
N_T	1 (247)	0.006	0.996	1 (270)	0.566	0.589	1 (269)	3.873	**0.004**	1 (220)	2.823	**0.008**
N_N	1 (246)	4.261	**0.001**	1 (269)	1.721	0.080	1 (268)	3.135	**0.006**	1 (219)	4.917	**0.002**
Comp	4 (242)	2.345	0.263	4 (265)	2.217	0.343	4 (264)	2.646	0.119	4 (215)	4.055	**0.014**

S.I.2. Estimating model parameters

In order to estimate the parameters for Eqs. 2-5 (in the main text), we fit a negative binomial generalised linear model to our observations of seed production for each of our four focal species separately. We did this regression in R (R Development Core Team, 2016), using the manyglm function from the mvabund package (Wang et al., 2012). For the baseline model (no environmental effect), the model formula was the following:

$$Fitness \sim \beta_0 + \beta_1 A + \beta_2 H + \beta_3 T + \beta_4 W + \beta_5 N$$

where 'Fitness' refers to our observations of seed production, β_0 is an intercept and 'A', 'H', 'T', 'W' and 'N' are the abundances of *A. calendula, H. glabra, T. cyanopetala, W. acuminata* and all other species in the immediate neighbourhood of the focal individual, respectively. β_0 gives us the value of $\tilde{\alpha}_i$ for intrinsic fitness in Eq. 3 (main text), whereas the coefficients for the abundances of each neighbour (β_1 - β_5) give us the equivalent interaction coefficients (α_{ii} and α_{ij} in Eqs. 4 and 5 in the main text).

For our environmental models, the model formula was:

$$Fitness \sim \beta_0 + \beta_1 abiotic + \beta_2 I(abiotic\text{^}2) + \beta_3 A + \beta_4 H + \beta_5 T + \beta_6 W + \beta_7 N + \beta_8 A{:}abiotic + \beta_9 H{:}abiotic + \beta_{10} T{:}abiotic + \beta_{11} W{:}abiotic + \beta_{12} N{:}abiotic + \beta_{13} A{:}I(abiotic\text{^}2) + \beta_{14} H{:}I(abiotic\text{^}2) + \beta_{15} T{:}I(abiotic\text{^}2) + \beta_{16} W{:}I(abiotic\text{^}2) + \beta_{17} N{:}I(abiotic\text{^}2)$$

The effect of environmental variation is included by adding both a linear ('abiotic') and quadratic ('I(abiotic^2)') term, as well as an interaction between each of these and the neighbouring species (e.g. 'A:abiotic' and 'A:I(abiotic^2)'). We use the coefficients estimated above to calculate the parameters for intrinsic fitness:

$$(1)\ \tilde{\alpha}_i = \beta_0 - \frac{{\beta_1}^2}{4\beta_2}$$

(2) $\tilde{b}_i = \beta_2$

(3) $\dot{\xi}_i = \frac{-\beta_1}{2\beta_2}$

Where β_0 in S.I. Eq. 1 refers to the intercept, and β_1 and β_2 refer to the coefficients estimated for the terms 'abiotic' and 'I(abiotic^2)'. Substituting S.I. Eqs. 1-3 into Eq. 3 (main text), we get:

(4) $\lambda_i = e^{\beta_0 - \frac{{\beta_1}^2}{4\beta_2} + \beta_2\left(\xi - \frac{-\beta_1}{2\beta_2}\right)^2}$

Which simplifies to:

(5) $\lambda_i = e^{\beta_0 + \beta_1\xi + \beta_2\xi^2}$

We proceed in the same manner for calculating the parameters for each of the interaction coefficients. For example, with species *j* as *H. glabra* we get:

(6) $\bar{\alpha}_{ij} = \beta_4 - \frac{{\beta_9}^2}{4\beta_{14}}$

(7) $\delta_{ij} = \beta_{14}$

(8) $\dot{\xi}_{ij} = \frac{-\beta_9}{2\beta_{14}}$

Substituting S.I. Eqs. 6-8 into Eq. 5 (main text) simplifies to:

(9) $\alpha_{ij} = \beta_4 + \beta_9\xi + \beta_{14}\xi^2$

S.I.3. Estimates model parameters

Supplementary Figure 3.1: Summary graph of estimated parameters for the focal species *A. calendula* varying along gradients of tree canopy cover, phosphorus and water availability.

The top row (a-c) shows estimates of intrinsic fitness λ_i, and the second row (d-f) shows intraspecific interaction strength α_{ii} (Eq. 4 in the main text). The three bottom rows show how estimates of interspecific interaction strength α_{ij} (Eq. 5 in the main text) between *A. calendula* and each of the other three focal species (g-i: *W. acuminata*; j-l: *T. cyanopetala*; m-o: *H. glabra*) vary along each gradient. In the graphs depicting interaction strength (d-o), any value over 0 (in white) indicates competition, and any value below 0 (in grey) indicates facilitation. Lines represent model fits and dotted lines give the simulated 95% confidence intervals. The vertical dashed line present in the intrinsic fitness plots corresponds to the maximum or minimum environmental value (as determined by fecundity rather than abundance) for *A. calendula* given by ξ_i. The darker ticks along the x axis indicate where observations of fecundity collected along each environmental gradient.

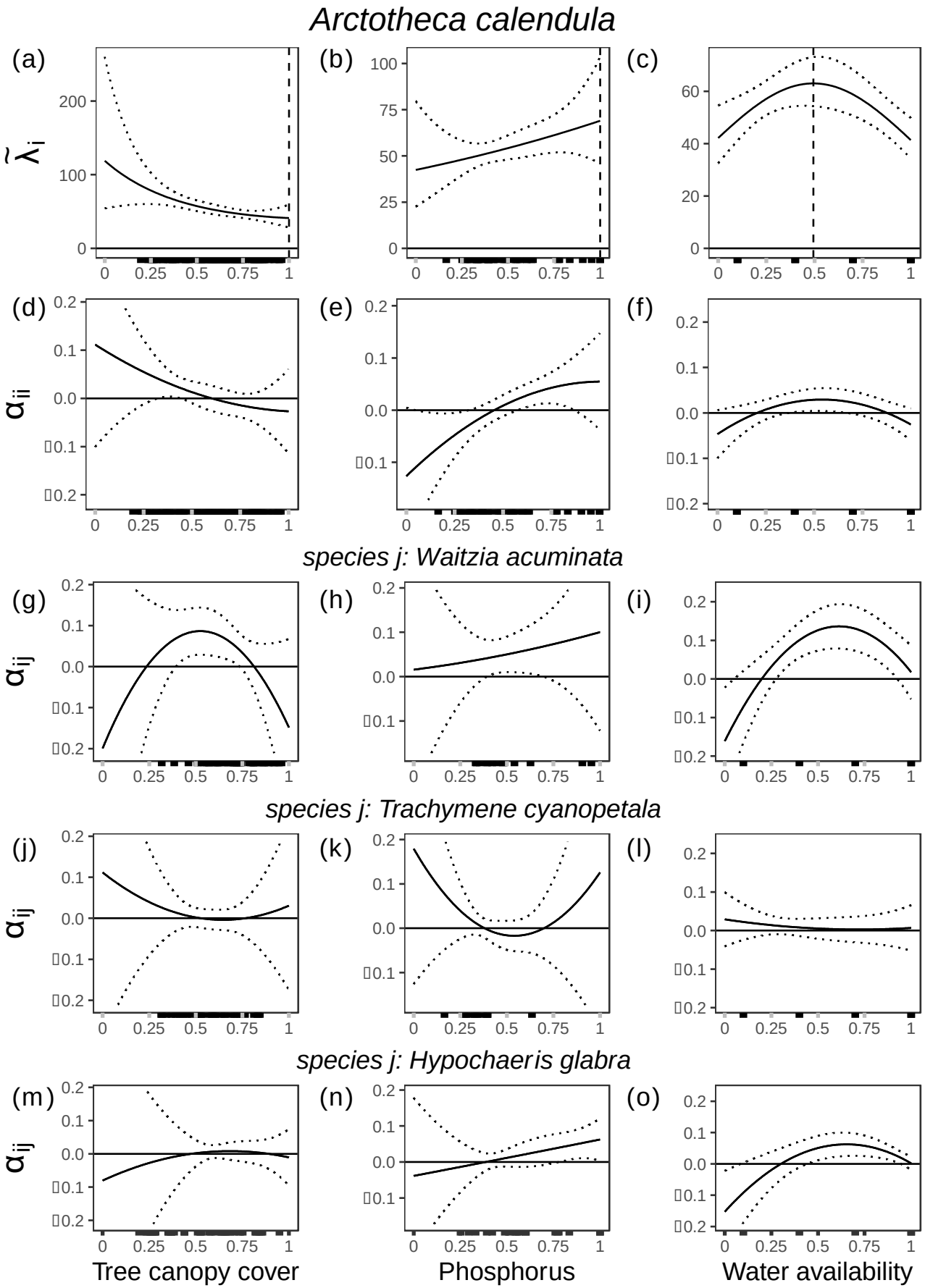
Arctotheca calendula
(a)
(b)
(c)
(d)
(e)
(f)
species j: Waitzia acuminata
(g)
(h)
(i)
species j: Trachymene cyanopetala
(j)
(k)
(l)
species j: Hypochaeris glabra
(m)
(n)
(o)
Tree canopy cover
Phosphorus
Water availability

78

79

Supplementary Figure 3.2: Summary graph of estimated parameters for the focal species *H. glabra* varying along gradients of tree canopy cover, phosphorus and water availability.

The top row (a-c) shows estimates of intrinsic fitness λ_i, and the second row (d-f) shows intraspecific interaction strength α_{ii}(Eq. 4 in the main text). The three bottom rows show how estimates of interspecific interaction strength α_{ij} (Eq. 5 in the main text) between *H. glabra* and each of the other 3 focal species (g-i: *W. acuminata;* j-l: *T. cyanopetala*; m-o: *A. calendula*) vary along each gradient. In the graphs depicting interaction strength (d-o), any value over 0 (in white) indicates competition, and any value below 0 (in grey) indicates facilitation. Lines represent model fits and dotted lines give the simulated 95% confidence intervals. The vertical dashed line present in the intrinsic fitness plots corresponds to the maximum or minimum environmental value (as determined by fecundity rather than abundance) for *H. glabra* given by ξ_i. The darker ticks along the x axis indicate where observations of fecundity collected along each environmental gradient.

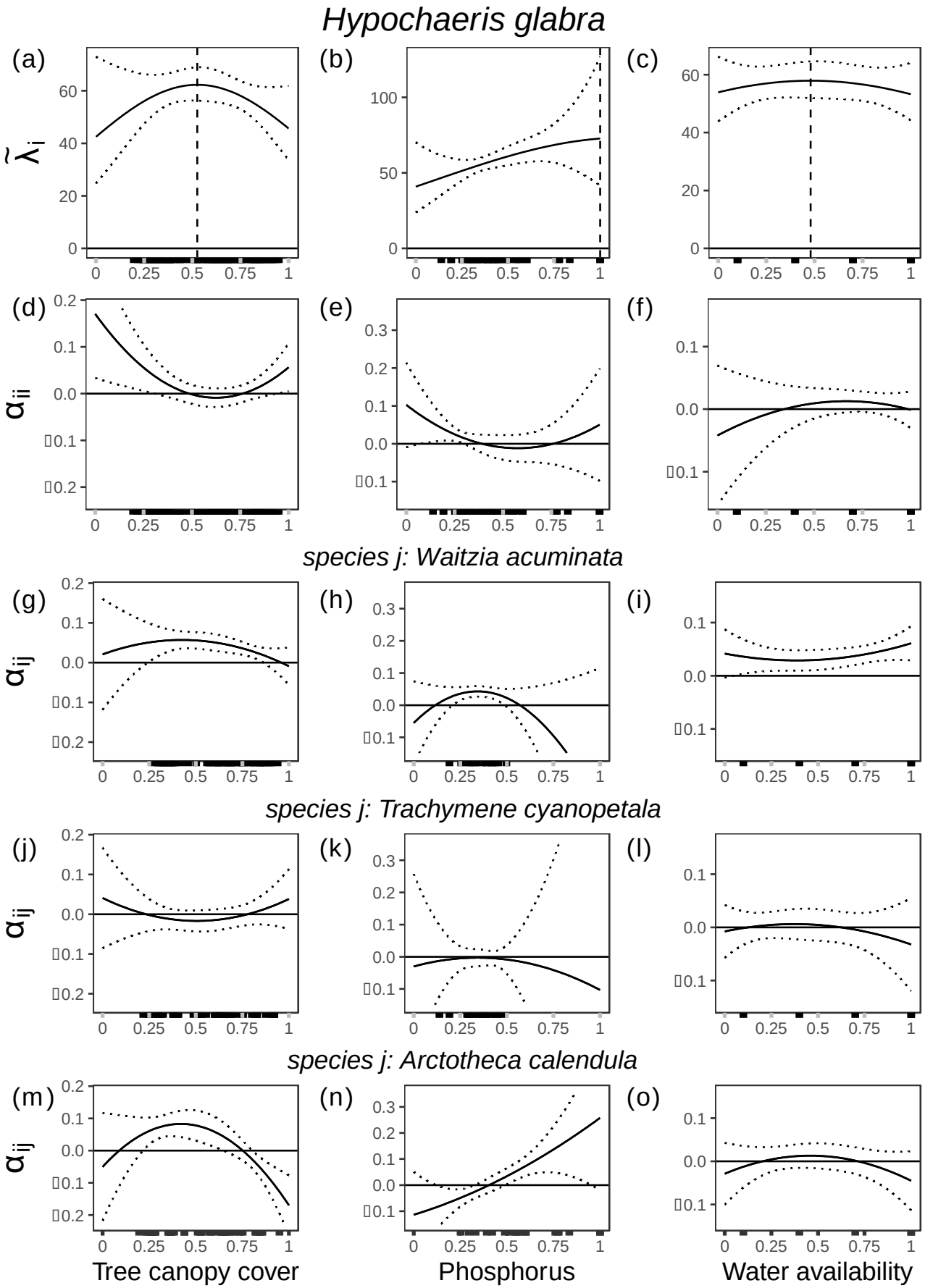
Hypochaeris glabra
(a)
(b)
(c)
(d)
(e)
(f)
species j: Waitzia acuminata
(g)
(h)
(i)
species j: Trachymene cyanopetala
(j)
(k)
(l)
species j: Arctotheca calendula
(m)
(n)
(o)
Tree canopy cover
Phosphorus
Water availability

94

Supplementary Figure 3.3: Summary graph of estimated parameters for the focal species *T. cyanopetala* varying along gradients of tree canopy cover, phosphorus and water availability.

The top row (a-c) shows estimates of intrinsic fitness λ_i, and the second row (d-f) shows intraspecific interaction strength α_{ii}(Eq. 4 in the main text). The three bottom rows show how estimates of interspecific interaction strength α_{ij} (Eq. 5 in the main text) between *T. cyanopetala* and each of the other 3 focal species (g-i: *W. acuminata*; j-l: *H. glabra*; m-o: *A. calendula*) vary along each gradient. In the graphs depicting interaction strength (d-o), any value over 0 (in white) indicates competition, and any value below 0 (in grey) indicates facilitation. Lines represent model fits and dotted lines give the simulated 95% confidence intervals. The vertical dashed line present in the intrinsic fitness plots corresponds to the maximum or minimum environmental value (as determined by fecundity rather than abundance) for *T. cyanopetala* given by $\acute{\xi}_i$. The darker ticks along the x axis indicate where observations of fecundity collected along each environmental gradient.

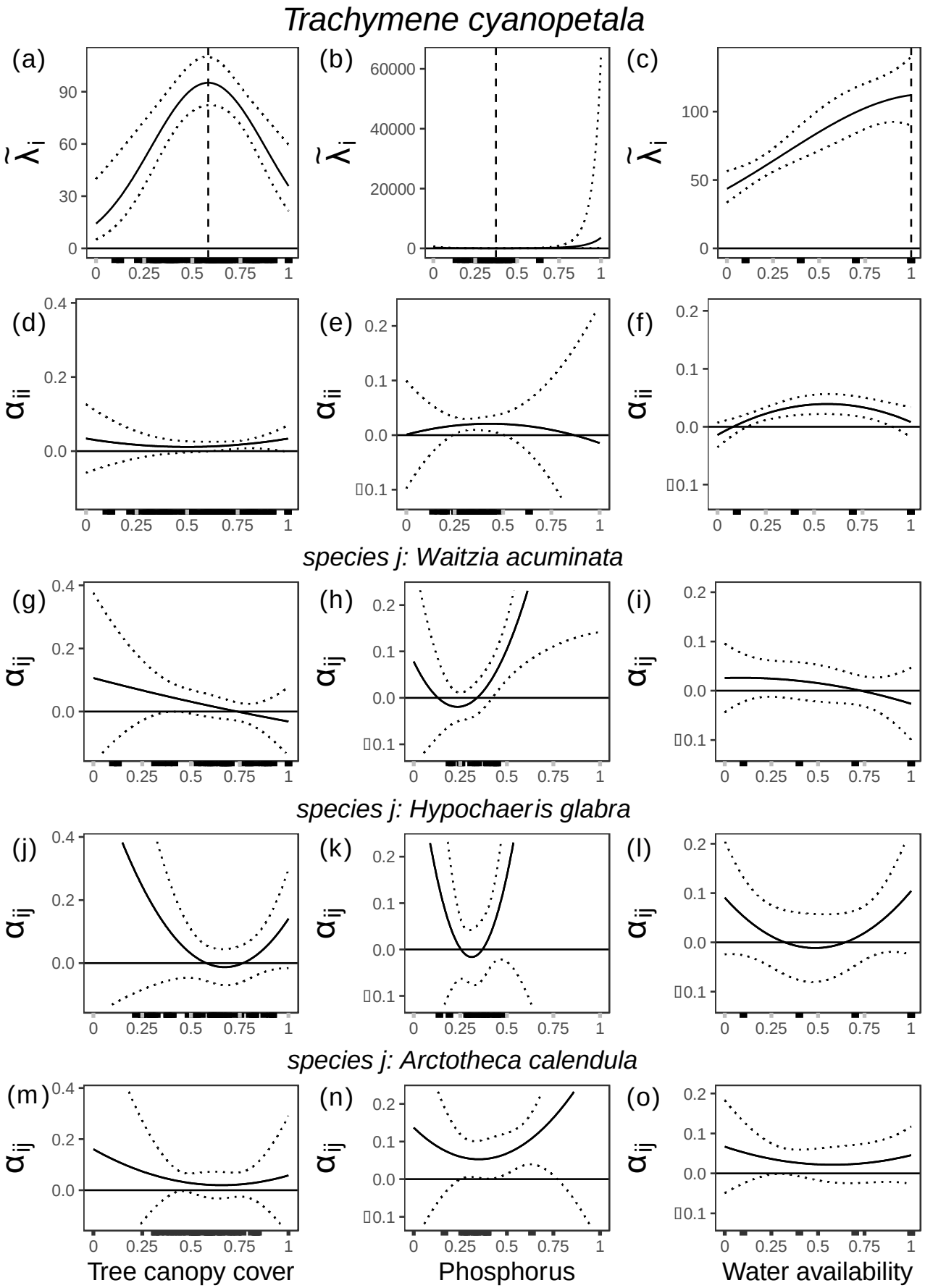
Trachymene cyanopetala
(a)
(b)
(c)
(d)
(e)
(f)
species j: Waitzia acuminata
(g)
(h)
(i)
species j: Hypochaeris glabra
(j)
(k)
(l)
species j: Arctotheca calendula
(m)
(n)
(o)
Tree canopy cover
Phosphorus
Water availability

109

Supplementary Figure 3.4: Summary graph of estimated parameters for the focal species *W. acuminata* varying along gradients of tree canopy cover, phosphorus and water availability.

The top row (a-c) shows estimates of intrinsic fitness λ_i, and the second row (d-f) shows intraspecific interaction strength α_{ii} (Eq. 4 in the main text). The three bottom rows show how estimates of interspecific interaction strength α_{ij} (Eq. 5 in the main text) between *W. acuminata* and each of the other 3 focal species (g-i: *T. cyanopetala*; j-l: *H. glabra*; m-o: *A. calendula*) vary along each gradient. In the graphs depicting interaction strength (d-o), any value over 0 (in white) indicates competition, and any value below 0 (in grey) indicates facilitation. Lines represent model fits and dotted lines give the simulated 95% confidence intervals. The vertical dashed line present in the intrinsic fitness plots (a-c) corresponds to the maximum or minimum environmental value (as determined by fecundity rather than abundance) for *W. acuminata* given by ξ_i. The darker ticks along the x axis indicate where observations of fecundity collected along each environmental gradient.

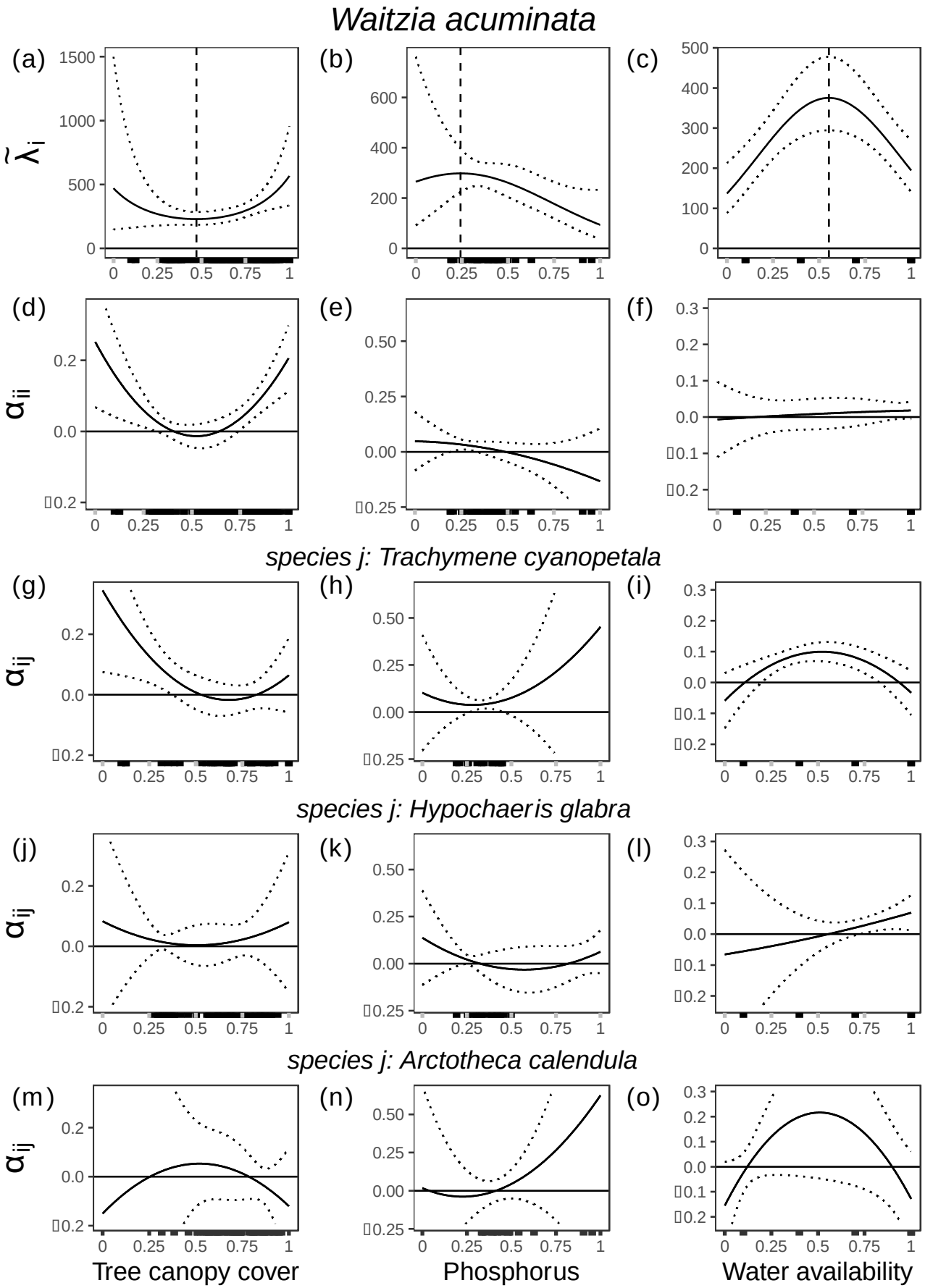
Waitzia acuminata
(a)
(b)
(c)
(d)
(e)
(f)
species j: Trachymene cyanopetala
(g)
(h)
(i)
species j: Hypochaeris glabra
(j)
(k)
(l)
species j: Arctotheca calendula
(m)
(n)
(o)
Tree canopy cover
Phosphorus
Water availability

123

S.I.4. Scaling the interactions

In modern coexistence theory, Chesson (2000b) defined niche overlap and fitness differences from the following Lotka-Volterra model:

$$\frac{1}{N_i}\frac{dN_i}{dt} = r_i\left(1 - \alpha_{ii}N_i - \alpha_{ij}N_j\right) \quad (10)$$

The rate of change in the abundance of species i, N_i, is determined by its intrinsic rate of increase r_i. Here, the interaction coefficients $\alpha_{..}$ are directly proportional to the abundance of competing individuals. In the case of our annual plant model (Eqs. 1 and 2 in the main text) however, the $\alpha_{..}$ are also proportional to intrinsic fitness λ_i and to the germination rates g_i and g_j.

In order to calculate niche overlap and fitness differences, we rescale the $\alpha_{..}$'s in our model to more closely resemble those in Chesson's Lotka-Volterra model. This step means that the interaction coefficients are no longer proportional to intrinsic fitness or germination rates and are instead directly proportional to the abundance of competing individuals (see Appendix A in Godoy & Levine, 2014 for a similar approach). This approach involves including intrinsic fitness and germination rates into the rescaled interaction coefficients ($\alpha'_{..}$) in such a way that these variables are cancelled out when we replace the $\alpha_{..}$s in our annual plant population model with $\alpha'_{..}$ and simplify.

We define β_i as the loss rate of seeds in the seed bank, and η_i as the productivity, i.e. the annual seed production per seed lost from the seed bank.

$$\beta_i = 1 - (1 - g_i)(s_i) \quad (11)$$

$$\eta_i = \frac{\lambda_i g_i}{\beta_i} \quad (12)$$

We can then rescale the $\alpha_{..}$ by defining $\alpha'_{..}$:

146 (13) $$\alpha_{ii}{}' = \frac{g_i \alpha_{ii}}{ln(\eta_i)} = \frac{g_i\left(\bar{\alpha}_{ii} + \delta_{ii}(\xi - \xi_{ii})^2\right)}{ln(\eta_i)}$$

147 and

148 (14) $$\alpha_{ij}{}' = \frac{g_j \alpha_{ij}}{ln(\eta_i)} = \frac{g_j\left(\bar{\alpha}_{ij} + \delta_{ij}(\xi - \xi_{ij})^2\right)}{ln(\eta_i)}$$

149 This allows us to rewrite our annual plant population model such that the $\alpha'_{..}$ have an
150 analogous effect on plant fitness as the interaction coefficients in Chesson's original Lotka -
151 Volterra model:

152 (15) $$\frac{N_{i,t+1}}{N_{i,t}} = (1 - \beta_i) + \beta_i \eta_i e^{-ln(\eta_i)(\alpha'_{ii} N_{i,t} + \alpha'_{ij} N_{j,t})}$$

153 To confirm that these rescaled interaction coefficients in this annual plant model are similarly
154 meaningful, we can check that they verify the invasibility criterion, such that for species *i* to
155 invade species *j* when *j* is at equilibrium, *j* must limit itself more than it limits *i* ($\alpha'_{jj} > \alpha'_{ij}$).

156 First, we determine $\dot{N}_j$, the density of species *j* when it is at equilibrium and in the absence of
157 species *i:*

158 (16) $$\dot{N}_j = \frac{ln(\eta_j)}{g_j \alpha_{jj}}$$

159 We then substitute $\dot{N}_j$ for $N_{j,t}$ in our annual plant model (Eq. 1 in the main text), rewriting it to
160 include β_i and η_i and assuming that there are no competing individuals of species *i:*

161 (17) $$\frac{N_{i,t+1}}{N_{i,t}} = (1 - \beta_i) + \beta_i \eta_i e^{-\alpha_{ij} g_j \frac{ln(\eta_j)}{g_j \alpha_{jj}}}$$

162 This gives us the growth rate of species *i,* which must be over 1 for it to invade:

163 (18) $$1 < (1 - \beta_i) + \beta_i \eta_i e^{-\alpha_{ij} g_j \frac{ln(\eta_j)}{g_j \alpha_{jj}}}$$

164 which simplifies to:

165 (19) $$\frac{g_j \alpha_{jj}}{ln(\eta_j)} > \frac{g_j \alpha_{ij}}{ln(\eta_i)}$$

166

S.I.5. Defining niche overlap and fitness differences

Chesson (2012) defined niche overlap as:

$$\rho = \sqrt{\frac{\alpha_{ij}\alpha_{ji}}{\alpha_{jj}\alpha_{ii}}} \quad (20)$$

Chesson & Kuang (2008) defined the average fitness difference as:

$$\frac{\kappa_j}{\kappa_i} = \frac{\alpha_{ij}}{\alpha_{jj}}\left(\frac{1}{\rho}\right) = \sqrt{\frac{\alpha_{ij}\alpha_{ii}}{\alpha_{jj}\alpha_{ji}}} \quad (21)$$

We can begin by substituting the interaction coefficients in S.I.5. Eq. 20 and 21 with our rescaled $\alpha'_{..}$ (S.I.4. Eqs. 13 – 14). The same approach is used by Godoy & Levine (2014), though they are able to simplify their expressions such that niche overlap becomes a function of the unscaled interaction coefficients, and fitness differences, a function of the unscaled interaction coefficients and the seed productivities of species *i* and *j.* Here, we use a different annual plant population model which requires a different rescaling of the interaction coefficients, and this simplification is no longer applicable. We therefore continue to use the rescaled interaction coefficients $\alpha'_{..}$ throughout our study.

Our expressions, however, are still not mathematically tractable if any of the $\alpha'_{..}$s hold a negative value (indicating a facilitative interaction). We therefore remove the square root and exponentiate the $\alpha'_{..}$ such that facilitative interactions can be accounted for and ρ and $\frac{\kappa_j}{\kappa_i}$ don't blow-up when any $\alpha'_{..}$ in the denominator reaches 0.

In Chesson's framework, niche overlap reflects the ratio of inter- to intra specific interactions, whereas fitness differences reflect how species differ in their relative responses to interactions. Importantly, our exponentiated values hold the same meaning as above since the inequality in S.I.4. Eq. 19 still holds as:

$$e^{\frac{g_j\alpha_{jj}}{ln(\eta_j)}} > e^{\frac{g_j\alpha_{ij}}{ln(\eta_i)}} \quad (22)$$

S.I.6. Predicting coexistence

When all rescaled interaction coefficients α_{ij}' were competitive, we were able to calculate traditional measures of niche overlap (ρ) and fitness differences ($\frac{\kappa_j}{\kappa_i}$) as defined by Chesson (2000b) and Chesson & Kuang (2008). We did this by substituting the interaction coefficients in his expressions with our rescaled α_{ij}' as shown in equations 23 and 24 below:

$$\rho = \sqrt{\frac{\alpha_{ij}'\alpha_{ji}'}{\alpha_{ii}'\alpha_{jj}'}} \quad (23)$$

$$\frac{\kappa_j}{\kappa_i} = \sqrt{\frac{\alpha_{ij}'\alpha_{ii}'}{\alpha_{jj}'\alpha_{ji}'}} \quad (24)$$

Coexistence between a pair of species is predicted when $\rho < \frac{\kappa_j}{\kappa_i} < \frac{1}{\rho}$. Supplemental Table 2 shows how often we were able to calculate traditional niche overlap and fitness differences from our predictions of interaction coefficients, and when those calculations resulted in predicted coexistence.

Supplementary Figures 6.1 and 6.2 are two examples of the patterns we observed in terms of the relative contributions of niche overlap and fitness differences to coexistence among focal species pairs in this study. In Supp. Fig 6.1, *H. glabra* and *W. acuminata* move further away from the space where coexistence is predicted (defined by the grey cone) as phosphorus concentration increases. In Figure 6.2, niche overlap and fitness differences between *W. acuminata* and *H. glabra* shift non-monotypically as tree canopy cover increases, eventually predicting coexistence in highly shaded plots.

Model type	Environmental variable	N total	N coexistence	N predicted	Details
Baseline	NA	12	8	0	
Environmental	Canopy	251	59	3	*H. glabra & W. acuminata*
	Phosphorus	82	18	0	
	Water	24	9	1	*A. calendula & T. cyanopetala*

Supplementary Table 6.1: Summary of our predicted coexistence outcomes. Model type refers to the model formulation described in the Methods under "Model framework". 'N total' refers to the total number of observations made, 'N coexistence' is the number of observations where coexistence outcomes can be predicted (in other words, when all interactions are competitive) and 'N predicted' is the number of observations for which we did predict coexistence to occur ($\rho < \frac{\kappa_j}{\kappa_i} < \frac{1}{\rho}$).

Parameters for the baseline model are fixed across the environmental gradient. This is why there are only 12 total observations (1 for each species pair). In the environmental models, intrinsic fitness (λ_i) and all interaction coefficients ($\alpha_{..}'$) can vary, such that predictions are calculated whenever a species pair shares the same environmental context (i.e. when they share a given value for any one environmental variable (ξ)). We limited our predictions to environmental values to the environmental space for which we had observational data (excluding the modelled tails evident in S.I.3. Figs. 3.1-3.4).

Supplementary Figure 6.1: Coexistence plot between *Hypochaeris glabra* and *Waitzia acuminata*. Niche overlap (ρ) is plotted on the x- axis, and fitness differences ($\frac{\kappa_j}{\kappa_i}$) on the y- axis. The region of the graph where these species are predicted to coexist is shown in grey and is defined by the inequality $\rho < \frac{\kappa_j}{\kappa_i} < \frac{1}{\rho}$. Each dot represents a prediction for a given value of ground phosphorus, with dots increasing in size as phosphorus concentration increases.

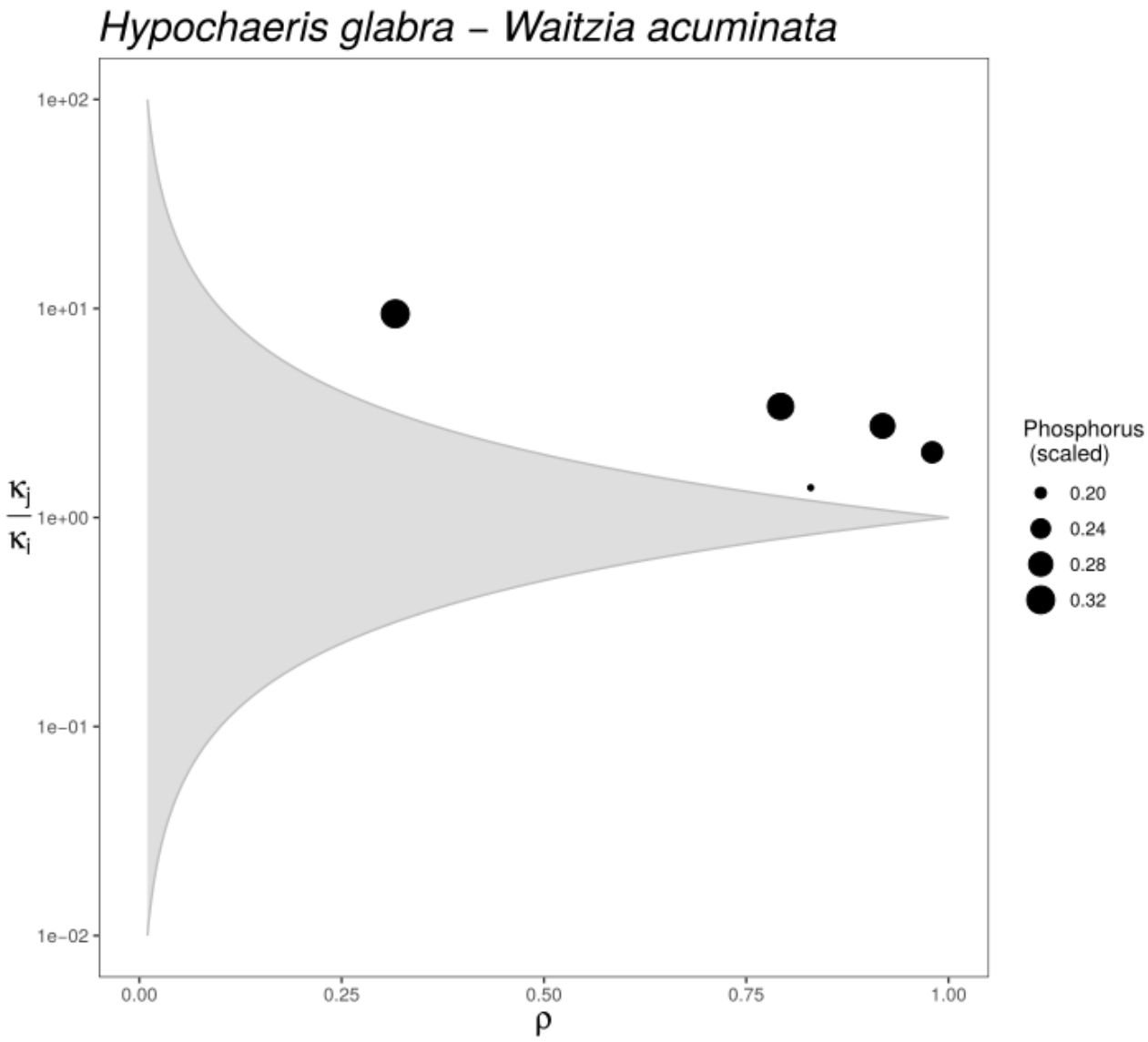

Supplementary Figure 6.2: Coexistence plot between *Waitzia acuminata* and *Hypochaeris glabra*. Niche overlap (ρ) is plotted on the x- axis, and fitness differences ($\frac{\kappa_j}{\kappa_i}$) on the y- axis. The region of the graph where these species are predicted to coexist is shown in grey and is defined by the inequality $\rho < \frac{\kappa_j}{\kappa_i} < \frac{1}{\rho}$. Each dot represents a prediction for a given value of tree canopy cover, with dots increasing in size as canopy cover increases. In addition, dots are numbered in increasing value of tree canopy cover to better illustrate the threshold observed between values 7 and 8.

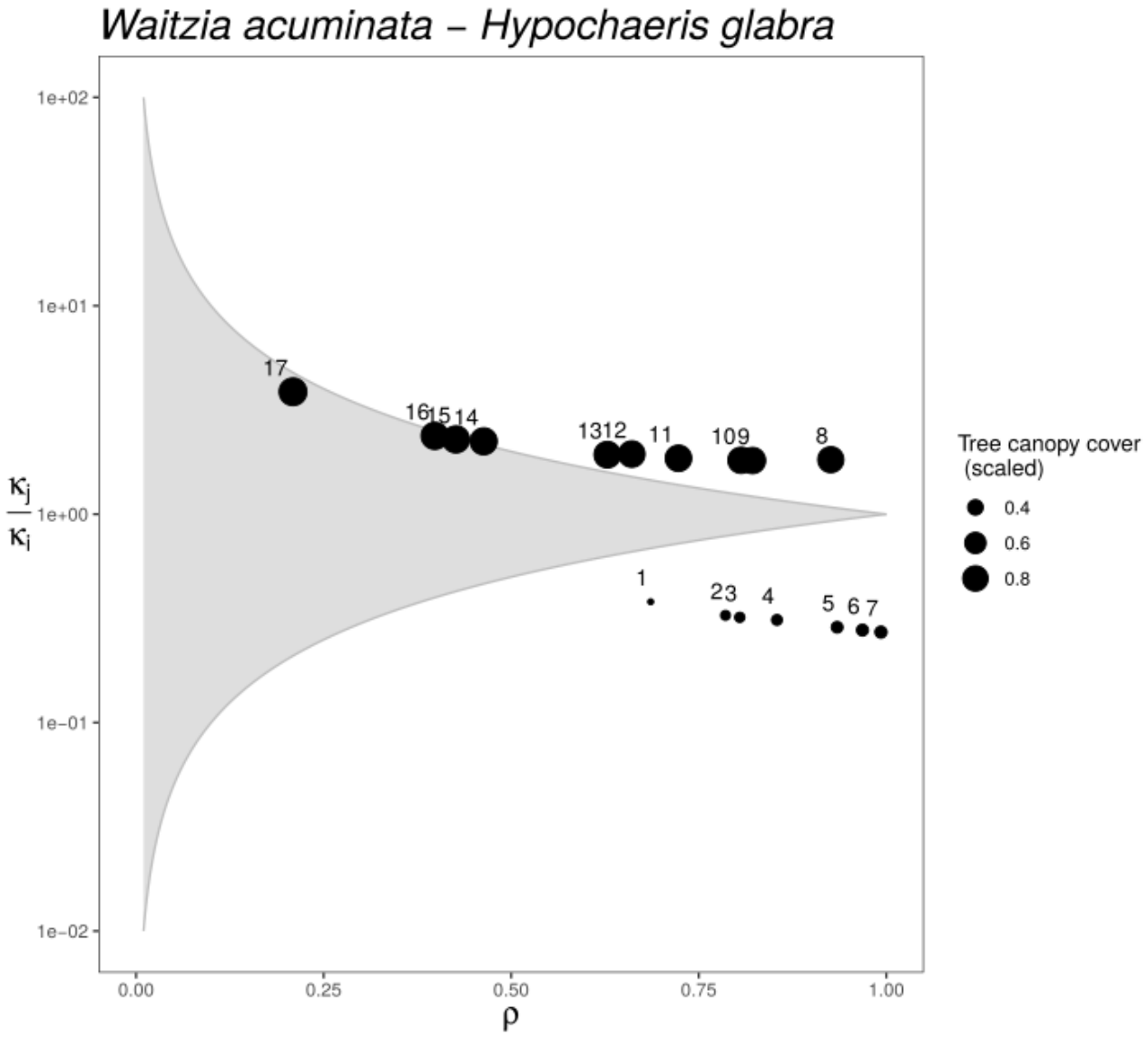

S.I.7. Niche overlap and fitness differences

Supplementary Figure 7.1: Predicted variation in our analogues of niche overlap (ρ, Eq. 11 in the main text) in black, and fitness differences ($\frac{\kappa_j}{\kappa_i}$, Eq. 12 in the main text) in grey, along each environmental gradient between *A. calendula* and the other three focal species. The two lines for each expression represent predicted values for each of the two reserves, which had different germination and seed survivability rates (see main Methods).

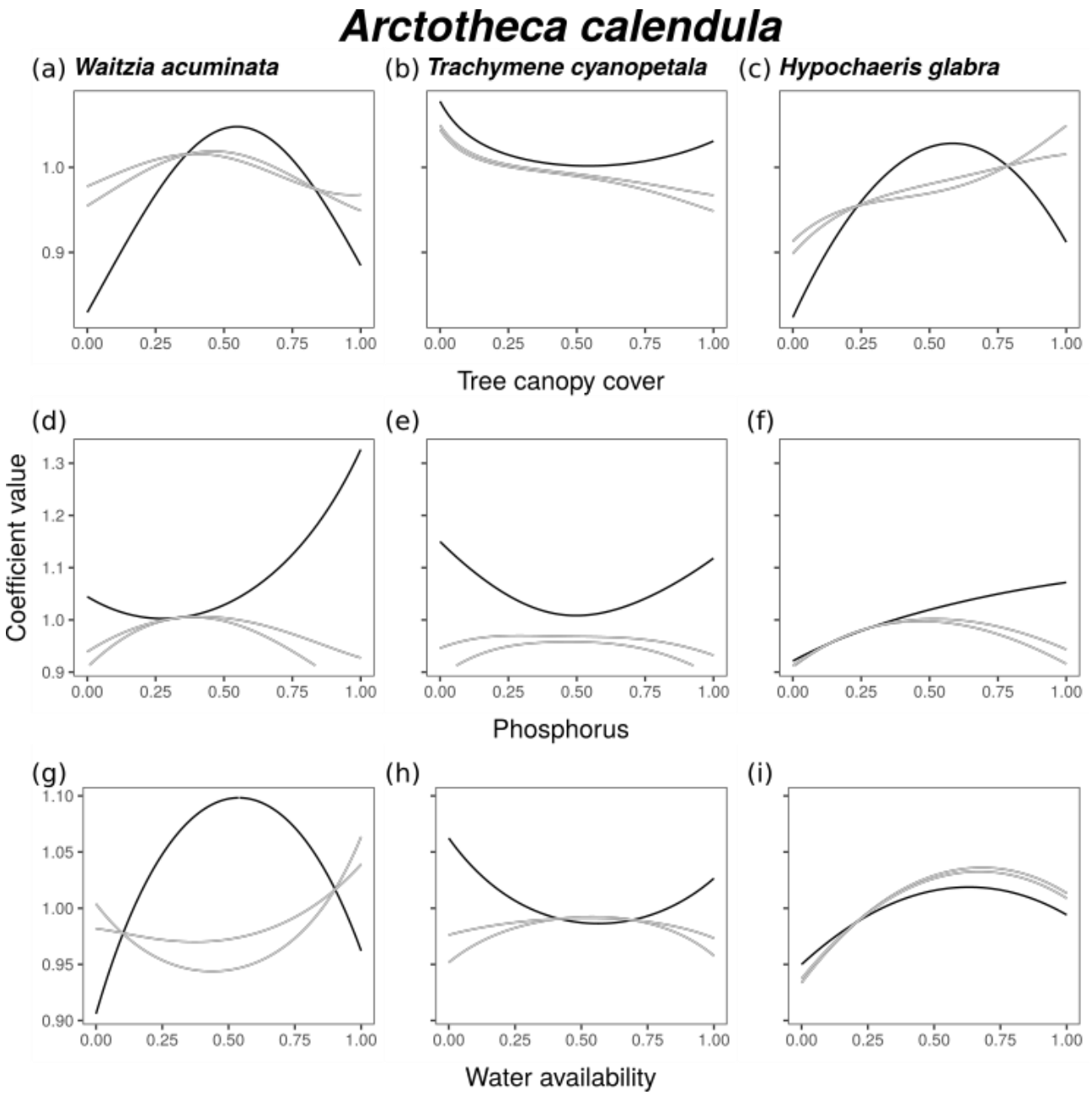

Supplementary Figure 7.2: Predicted variation in our analogues of niche overlap (ρ, Eq. 11 in the main text) in black, and fitness differences ($\frac{\kappa_j}{\kappa_i}$, Eq. 12 in the main text) in grey, along each environmental gradient between *H. glabra* and the other three focal species. The two lines for each expression represent predicted values for each of the two reserves, which had different germination and seed survivability rates (see main Methods).

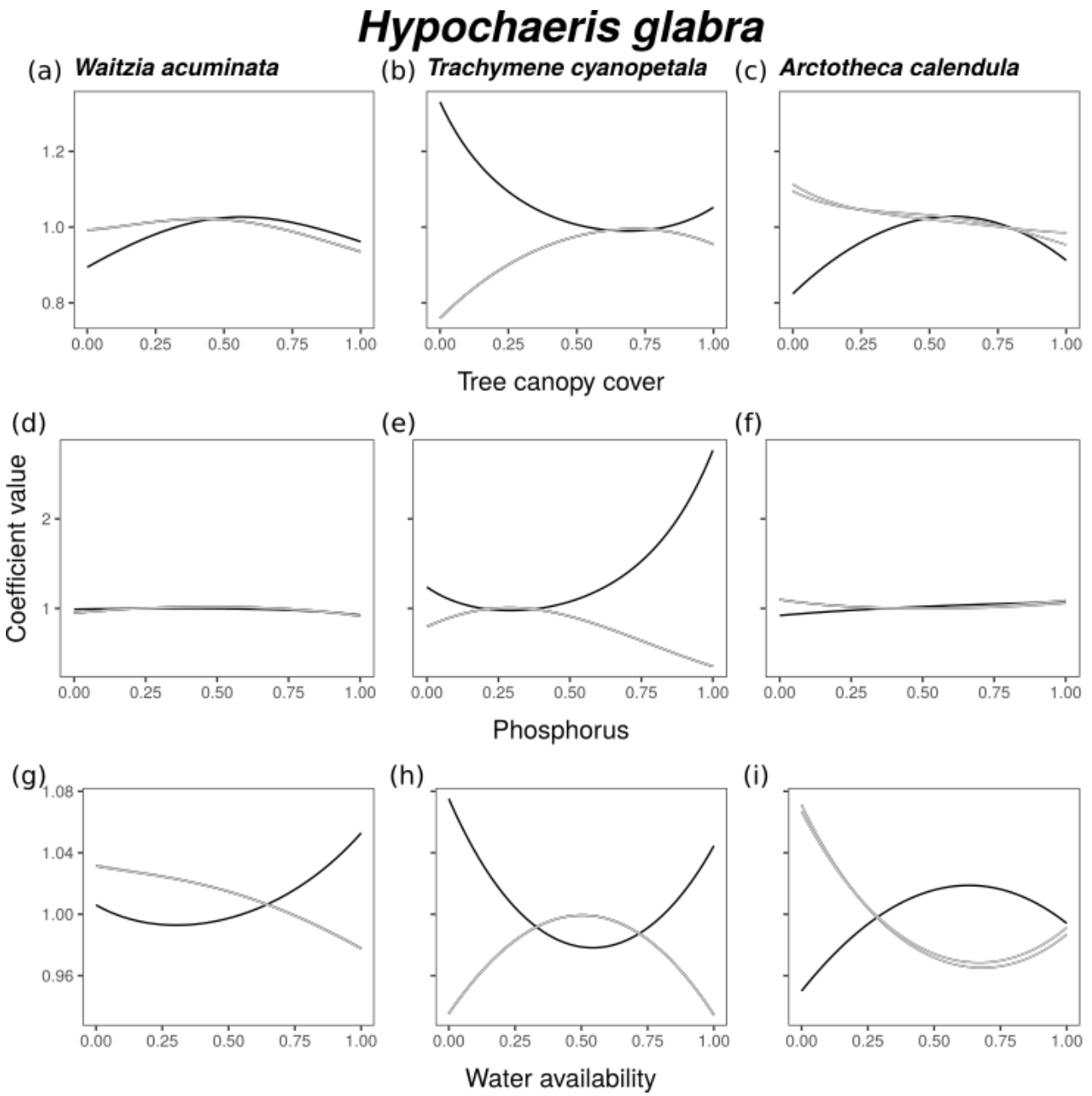

Supplementary Figure 7.3: Predicted variation in our analogues of niche overlap (ρ, Eq. 11 in the main text) in black, and fitness differences ($\frac{\kappa_j}{\kappa_i}$, Eq. 12 in the main text) in grey, along each environmental gradient between *T. cyanopetala* and each of the three other focal species. The two lines for each expression represent predicted values for each of the two reserves, which had different germination and seed survivability rates (see main Methods).

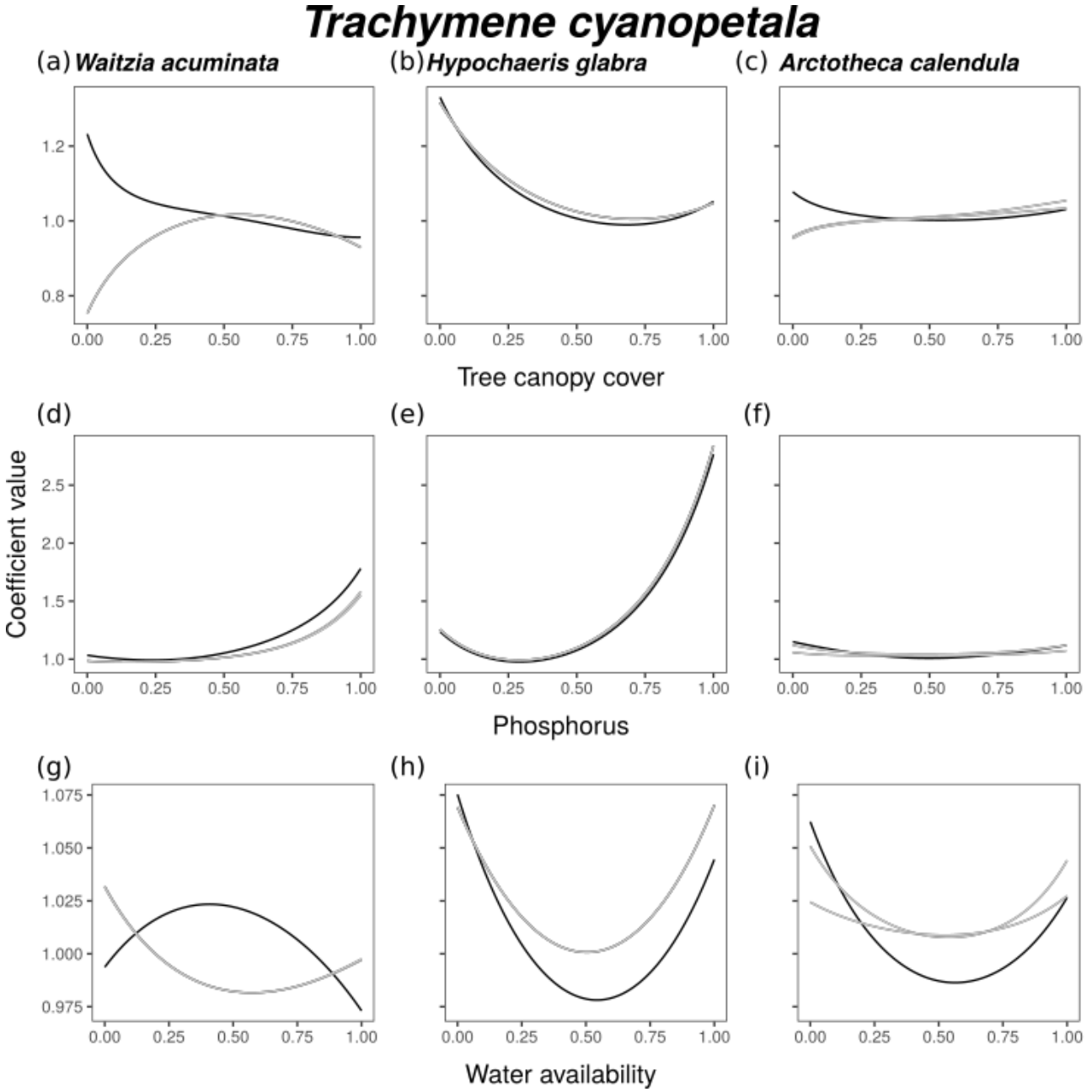

Supplementary Figure 7.4: Predicted variation in our analogues of niche overlap (ρ, Eq. 11 in the main text) in black, and fitness differences ($\frac{\kappa_j}{\kappa_i}$, Eq. 12 in the main text) in grey, along each environmental gradient between *W. acuminata* and the other three focal species. The two lines for each expression represent predicted values for each of the two reserves, which had different germination and seed survivability rates.

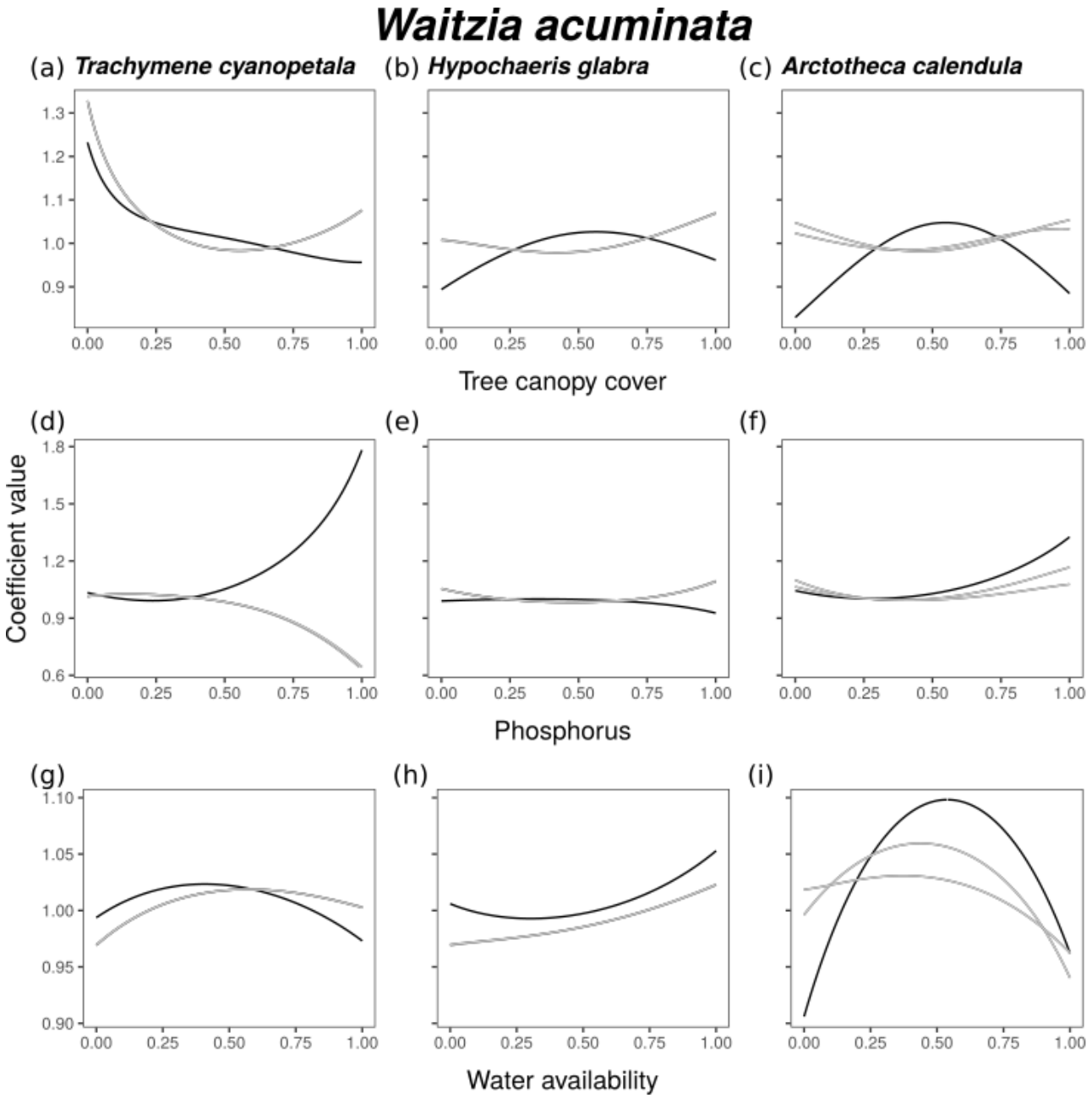

Reference List

Chesson, P. (2000). Mechanisms of maintenance of species diversity. *Annual Review of Ecology and Systematics*, *31*, 343–66. http://doi.org/10.1146/annurev.ecolsys.31.1.343

Chesson, P. (2012). Species Competition and Predation. In R. Leemans (Ed.), *Ecological Systems* (pp. 223–256). New York, NY: Springer.

Chesson, P., & Kuang, J. J. (2008). The interaction between predation and competition. *Nature*, *456*(7219), 235–238. http://doi.org/10.1038/nature07248

Godoy, O., & Levine, J. M. (2014). Phenology effects on invasion success: Insights from coupling field experiments to coexistence theory. *Ecology*, *95*(3), 726–736. http://doi.org/10.1890/13-1157.1

R Development Core Team. (2016). R: A Language and Environment for Statistical Computing. *R Foundation for Statistical Computing Vienna Austria*, *0*.

Wang, Y., Naumann, U., Wright, S. T., & Warton, D. I. (2012). Mvabund- an R package for model-based analysis of multivariate abundance data. *Methods in Ecology and Evolution*, *3*(3), 471–474. http://doi.org/10.1111/j.2041-210X.2012.00190.x